Journal of Power Sources 196 (2011) 6507–6511

Contents lists available at ScienceDirect

Journal of Power Sources

journal homepage: www.elsevier.com/locate/jpowsour

Short communication

High-strength all-solid lithium ion electrodes based on $Li_4Ti_5O_{12}$

Li Sun[a,b], Nikhil Karanjgaokar[c], Ke Sun[b], Ioannis Chasiotis[c], W. Craig Carter[a], Shen Dillon[b,*]

[a] Department of Materials Science and Engineering, Massachusetts Institute of Technology, Cambridge, MA 02139, United States
[b] Department of Materials Science and Engineering, University of Illinois at Urbana-Champaign, Urbana, IL 61801, United States
[c] Department of Aerospace Engineering, University of Illinois at Urbana-Champaign, Urbana, IL 61801, United States

ARTICLE INFO

Article history:
Received 29 January 2011
Received in revised form 17 March 2011
Accepted 23 March 2011
Available online 31 March 2011

Keywords:
Li-ion battery
Electrode
$Li_4Ti_5O_{12}$
Solid electrolyte
Strength
Sintering

ABSTRACT

A $Li_4Ti_5O_{12}$–$Li_{0.29}La_{0.57}TiO_3$–Ag electrode composite was fabricated via sintering the corresponding powder mixture. The process achieved a final relative density of 97% the theoretical. Relatively thick, ~100 μm, electrodes were fabricated to enhance the energy density relatively to the traditional solid-state thin film battery electrodes. The sintered electrode composite delivered full capacity in the first discharge at *C*/40 discharge rate. Full capacity utilization resulted from the 3D percolated network of both solid electrolyte and metal, which provide paths for ionic and electronic transport, respectively. The electrodes retained 85% of the theoretical capacity after 10 cycles at *C*/40 discharge rate. The tensile strength and the Young's modulus of the sintered electrode composite are the highest reported values to date, and are at least an order of magnitude higher than the corresponding value of traditional tapecast "composite electrodes". The results demonstrate the concept of utilizing thick all-solid electrodes for high-strength batteries, which might be used as multifunctional structural and energy storage materials.

1. Introduction

Gravimetric energy density and power density are amongst the most important metrics of battery performance [1–5]. This highlights the fact that, in the vast majority of applications, batteries are considered 'dead weight'. The importance of gravimetric energy density is demonstrated by considering the mass of the battery required to power a light-duty vehicle. Such an electric vehicle (EV) with a 150 mile all-electric range requires an approximately 45 kWh battery system. With current batteries delivering about 0.25 kWh kg^{-1}, the EV would require 180 kg battery pack. This represents 10–15% of the total mass of a light duty vehicle [3–5]. Ideally, energy storage media could replace massive components in a larger system, such that they perform multiple functions and their mass does not significantly contribute to that of the system.

Thomas and Qidwai [6] demonstrated traditional lithium ion batteries as structural components in micro-air vehicles. The integration improved the efficiency of these vehicles by increasing the energy to mass ratio of the vehicle. Unfortunately, traditional lithium ion batteries exhibit relatively poor mechanical properties, which limit their application as structural components.

Typical "composite electrodes" are composed of an active electrode material, percolating conductive carbons, and a binder phase [7]. The electrodes are cast and dried from slurry that leaves about 15–65% residual porosity [8,9]. The porous structure offers the conductive path for ionic transport. The conductive carbon diluents maintain electronic percolation. Unfortunately, inactive components, including binder, conductive carbon, current collectors, separators, and packaging, significantly limit the energy density of batteries. The active materials typically consist of less than 1/3 of the total volume and 1/2 of the total weight. The high porosity and addition of inactive components of the composite electrode also result in low tensile strength and low elastic modulus. The tensile strength and Young's modulus of a "composite electrode" have been reported to be ~4 MPa, and 0.2–0.7 GPa, respectively [10]. Packaged batteries have strengths on the order of 10 MPa [6].

Solid electrolytes, such as lithium lanthanum titanate ($Li_{0.29}La_{0.57}TiO_3$, LLTO) [11], and lithium aluminum titanium phosphate ($Li_{1.3}Al_{0.3}Ti_{1.7}(PO_4)_3$, LATP) [12], have lithium conductivities approaching those of liquid electrolytes. Solid electrolytes form the basis for thin film batteries. These batteries utilize dense ceramic films as electrodes separated by a thin solid electrolyte [13–15]. The diffusion coefficient of lithium in pure ceramic electrodes is relatively low at room temperature and certain electrodes also exhibit relatively low electronic conductivity [16]. The thicknesses of the electrodes are, therefore, limited to several micrometers. This limits the energy density of these batteries as they typically require a substrate much thicker than the batteries and packaging that is a large fraction of the total mass and volume.

* Corresponding author at: Department of Materials Science and Engineering, University of Illinois at Urbana-Champaign, 1304 W. Green St., Urbana, IL 61801, United States. Tel.: +1 217 244 5622; fax: +1 217 333 2736.
E-mail address: sdillon@illinois.edu (S. Dillon).

0378-7753/$ – see front matter © 2011 Elsevier B.V. All rights reserved.
doi:10.1016/j.jpowsour.2011.03.045

Table 1
The composition of various powder mixtures and the density of relative sintered samples.

Name	LTO:LLTO:Ag volumetric ratio	Density of sintered sample
LTO–LLTO–Ag	5:3:2	97.2 ± 1.3%
LTO–LLTO	7:3:0	82.1 ± 1.0%
LTO–Ag	8:0:2	98.1 ± 1.6%
LTO	1:0:0	93.2 ± 2.1%
LLTO–Ag (1)	0:8:2	88.3 ± 1.7%
LLTO–Ag (2)	0:5:5	94.6 ± 1.2%

Several studies have reported the fabrication of all-solid-state batteries, which contain solid composite electrodes [17–20]. The thickness of the electrode layer is between 4 and 60 μm. Unfortunately, no mechanical properties of relative solid electrodes/batteries were reported. Recently, Lai et al. [21] reported on sintered $LiCoO_2$ without additives as a cathode, which had 13–30% porosity for liquid electrolyte percolation, and provided high volumetric energy densities. This surprising result indicated that thick all-ceramic electrodes could be utilized reliably in spite of the volumetric strain associated with the system and the relatively low initial electronic conductivity of the stoichiometric compound.

Here, we report a new design of electrode with high-density (>97%) and relatively high-strength (~90 MPa) via standard powder processing and sintering. Fully inorganic electrodes consisting of active material ($Li_4Ti_5O_{12}$, LTO), solid electrolyte (LLTO), and metal (Ag) components were fabricated. This design is departure from the previous reports of all solid state electrodes [17–20]. In order to promote electronic and ionic percolation through the metal and the solid electrolyte a large volume fraction of these materials must be present. LLTO was selected as the solid electrolyte due to its high ionic conductivity. Silver was utilized as the electronic conductor due to its oxidation resistance during air annealing and its relatively low melting point (~960 °C) [22], which can promote densification. These sintered electrodes can be combined with either liquid or solid electrolyte to form Li-ion batteries. This offers a possibility to produce solid-state Li-ion batteries with high-strength, which can be used as the structural components in micro-air vehicles as discussed by Thomas and Qidwai [6], and may also be utilized as the package frame for the batteries in electric vehicle to increase the gravimetric energy density.

2. Experimental

LLTO was synthesized following the procedure report by Yoshiyuki et al. [11] from 99.99% pure rutile TiO_2 (Sigma–Aldrich Co., Inc., St. Louis, MO, USA), 99.3% pure Li_2CO_3 (L. T. Baker Chemical Co., Phillipsburg, NJ, USA), and 99.9% pure La_2O_3 (Acros Organics, NJ, USA). The synthesized LLTO was then ball-milled with 99.9% pure Ag (Strem Chemicals, Newburyport, MA, USA), and/or 99.9% pure $Li_4Ti_5O_{12}$ (Sigma–Aldrich Co., Inc., St. Louis, MO, USA) with 12-mm-diameter zirconia media in a polyethylene bottle for 48 h. Six powder mixtures were prepared with varying LTO–LLTO–Ag ratio, as listed in Table 1. The powder mixture was sieved through a 200 mesh screen and then compacted in a single-action die under 80 MPa. These green pellets were sintered at 950 °C for 1 h, which is in the liquid–solid transient sintering window of silver [23] and promotes sintering of the powder mixture.

The densities of the sintered electrodes were calculated by Archimedes' principle with ethanol as the media. The results are listed in Table 1. Phase analysis was performed via X-ray diffraction (XRD, Siemens-Bruker 5000, Bruker Axs Inc., Madison, WI, USA). Microstructures were observed by a scanning electron microscopy (JEOL 7000F, JEOL USA Inc., Peabody, MA, USA).

Sintered electrodes were ground to 92 ± 11 μm thickness and weighed (Mettler Toledo XP26, Mettler-Toledo Inc., Columbus, OH, USA) before cycling. The total mass and component mass fractions were used to calculate the electrode capacity. Each sintered electrode was tested against a Li counter electrode. A separator (CELGARD polymer) saturated with a 1 M $LiPF_6$ solution in ethylene carbonate and dimethyl carbonate (1:1) was used to assemble the batteries in a Swagelok-type cell. The cells were cycled using a potentiostat (SP200, Biologic SAS, Claix, France). The cell was cycled between 1 V and 2 V. In this voltage range, Besides Li^+/Li active redox couple, Ti^{4+}/Ti^{3+} may also be active, but Ag does not alloy with Li [24]. The charge rate was kept constant at $C/40$, while the discharge rate varied.

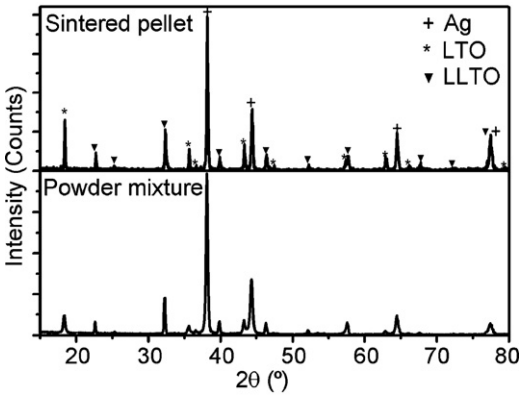

Fig. 1. XRD pattern of the LTO–LLTO–Ag powder mixture and the sintered LTO–LLTO–Ag electrode composite.

In order to characterize the mechanical properties of the electrode material, test specimens of rectangular cross-sections (W = 2.6 mm and t = 0.26 mm) and gauge length approximately L = 25 mm, with all six surfaces polished to 0.1 μm roughness with diamond suspensions were tested in uniaxial tension by using the mechanical testing apparatus described in [25]. The electrode composite samples were mounted on customized grips using high strength adhesives and the grips were then mounted onto the loading frame. The samples were then loaded in uniaxial tension until failure and the applied load was measured with a 25 lbs loadcell. A high resolution vertical camera system attached to an optical microscope objective of 50x magnification was used to record optical images at each successive step of loading. The optical images were then used for calculation of the specimen strain by digital image correlation (DIC) and then the stress-strain curves, from which, the effective elastic modulus and the tensile strength of the multiphase electrode material were obtained.

3. Results and discussion

3.1. Structural and phase characterization

The XRD patterns of the powder mixture and the sintered LTO/LLTO/Ag electrode are shown in Fig. 1. The XRD patterns show no obvious difference before and after sintering, containing only characteristic peaks of LTO, LLTO, and Ag. The ionic radius of Ag^+ (0.126 nm) is larger than both that of La^{3+} (0.116 nm) and the Ti^{4+} (0.068 nm). Ag^+ should be relatively insoluble in the lattice of LTO or LLTO. Therefore, the sintered electrode is a composite containing only the LTO, LLTO, and Ag component phases.

A backscatter electron (BSE) image of the sintered electrode in Fig. 2a confirms a three-phase composite structure. The average atomic weight decreases in the following order; Ag, LLTO, and LTO. Therefore, the brightest (white) grains are Ag, the darkest (black) grains are LTO, and the intermediate gray phase is LLTO. The relative density of sintered electrode was 97.2 ± 1.3%. Few pores are observed in Fig. 2, which are mainly associated with LTO grains.

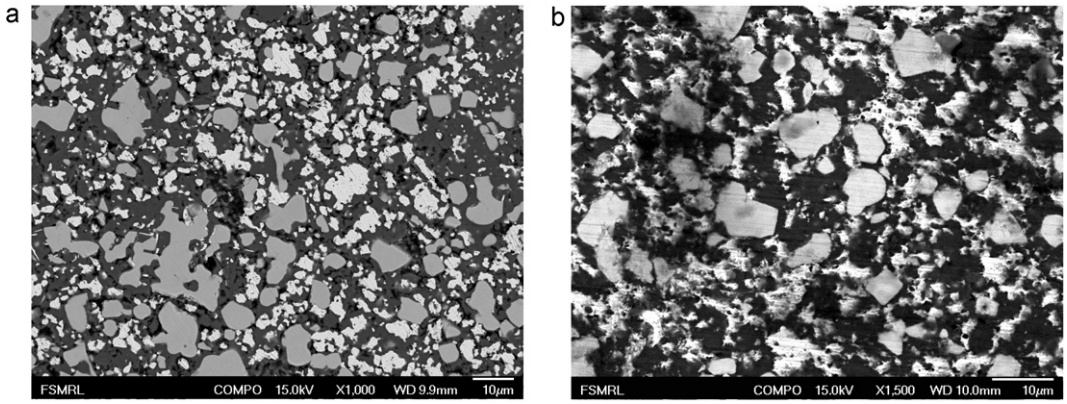

Fig. 2. Back-scatter electron (BSE) image of the sintering LTO–LLTO–Ag electrode composite: (a) before cycling, and (b) after 10 cycles.

During cycling, the intercalation and de-intercalation of Li-ion often induces stress/strain in the electrodes, resulting in the exfoliation [26]. However, spinel $Li_4Ti_5O_{12}$ exhibits no volumetric strain during charge–discharge cycling [27]. This likely limited mechanical failure in the sintered electrodes. After multiple cycles, the microstructure of the sintered electrode showed no obvious mechanical flaws or induced defects (Fig. 2b).

3.2. Electrochemical properties

Fig. 3 shows the charge–discharge curve of a sintered LTO–LLTO–Ag electrode composite at *C*/40 charge and discharge rates. The theoretical capacity of $Li_4Ti_5O_{12}$ is 175 mAh g^{-1} [28]. The sintered electrode composite achieved full capacity, as shown in Fig. 3. Fig. 4 shows discharge curves of a sintered LTO–LLTO–Ag electrode composite at different discharge rates. The measured capacity is slightly greater than theoretical capacity at *C*/40 discharge rate. This may result from slight differences in the intended and actual content of active material in the electrode. The discharge capacity decreased with increasing rate for all rates greater than *C*/40. Over 2/3 of the theoretical capacity was maintained at *C*/10, and approximately 1/3 of theoretical capacity remained at *C*/5. Traditional $Li_4Ti_5O_{12}$ composite electrodes based on nanoparticles maintain comparable capacities at rates approaching 4C [29]. However, the effective particle size of the $Li_4Ti_5O_{12}$ in the LTO–LLTO–Ag electrode composite is approximately 6.5 μm. Composite electrodes from micron scale $Li_4Ti_5O_{12}$ particles (~6 μm) [30] produced a similar discharge capacity to Fig. 4.

The $Li_4Ti_5O_{12}$, LTO/Ag, LLTO/Ag samples were discharged at *C*/40. There was almost no capacity for LLTO/Ag samples (~0.07 mAh g^{-1}). The initial discharge curves of the $Li_4Ti_5O_{12}$, LTO/Ag are compared to that of sintered LTO–LLTO–Ag electrode composite in Fig. 5. The LTO/LLTO sample does not make a useful direct comparison due to its relatively low density. Overall its capacity measured at *C*/40 discharge was approximately equivalent to the pure $Li_4Ti_5O_{12}$ sample (1.1 mAh g^{-1}). Clearly, the discharge capacity of the sintered LTO–LLTO–Ag electrode composite was much greater than sintered bulk $Li_4Ti_5O_{12}$, LTO–Ag, and LLTO–Ag composite. The thickness of the tested electrode pieces was 92 ± 11 μm. The low lithium diffusion coefficient and electronic conductivity of pure bulk $Li_4Ti_5O_{12}$ resulted in the lowest discharge capacity, as shown in Fig. 5. This comparison confirmed the design strategy for thick high-density high-strength fully inor-

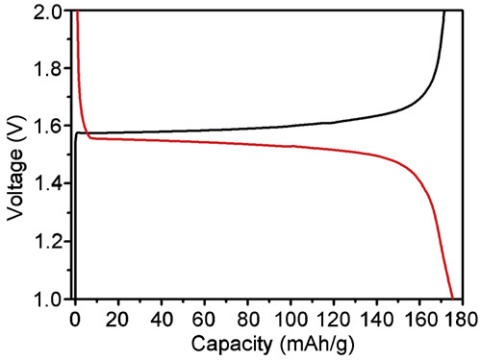

Fig. 3. Cycling behavior of a sintered LTO–LLTO–Ag electrode composite at *C*/40 scan rate; the capacities were calculated based on the mass of LTO.

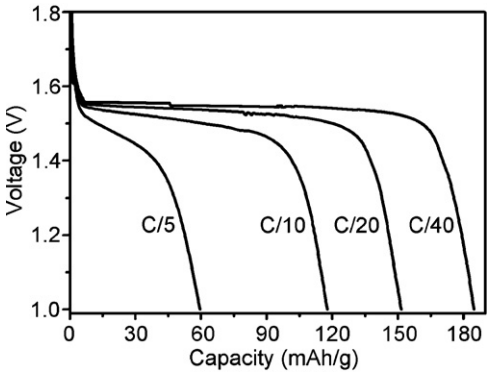

Fig. 4. Discharge curves of a sintered LTO–LLTO–Ag electrode composite at different current rates, the capacities were calculated based on the mass of LTO.

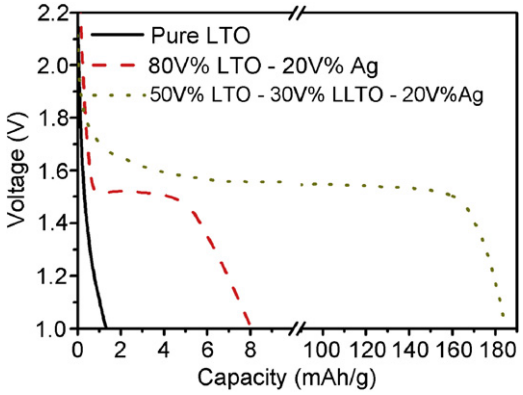

Fig. 5. Comparison of discharge curves of sintered bulk $Li_4Ti_5O_{12}$, LTO–Ag composite, and LTO–LLTO–Ag composite at *C*/40 scan rate; the capacities were calculated based on the mass of LTO.

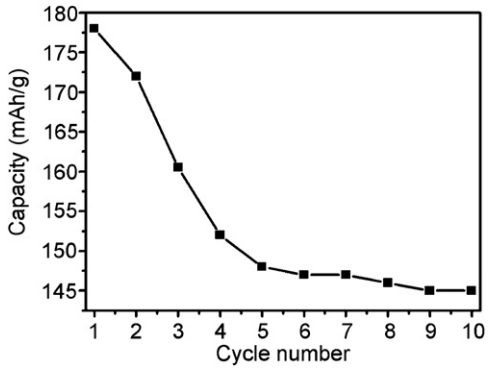

Fig. 6. Discharge capacities of the sintered LTO–LLTO–Ag electrode composite with the cycle number calculated based on the mass of LTO.

ganic electrodes: a percolating 3D network of both solid electrolyte and metal providing paths for ionic and electronic transport.

Capacity fade associated with the sintered LTO–LLTO–Ag electrodes cycled at *C*/40 charge/discharge rates is shown in Fig. 6. Significant initial capacity fade occurred with a decreasing rate of fade during subsequent cycles. The electrodes maintained approximately 85% of theoretical capacity after 10 cycles.

Although liquid electrolyte was used during electrochemical testing, the design of the LTO–LLTO–Ag electrode enables its use with a solid electrolyte, such as LLTO, to form all-solid-state Li-ion batteries. Similar, solid state electrodes with $LiCoO_2$, $LiMn_2O_4$, etc might be utilized for such batteries. Other metals can also sever as the electronic conductive filler, such as Au, Cu, Co, Ni, Al, stainless steel, etc. However, gold will increase the fabrication cost, and Cu, Co, Ni, and Al cannot be sintered in air due to oxidation. The control of sintering atmosphere is required to simultaneously preserve the oxidation states of the electronic conductor, the solid electrolyte, and the active electrode material. Related research is ongoing.

3.3. Mechanical properties

The average strength and the Young's modulus of the sintered LTO–LLTO–Ag electrode composite were measured to be 90 MPa, and 29 GPa, respectively. The Young's modulus of Ag is 83 GPa [31]. Although both LLTO and LTO are expected to have significantly higher Young's moduli than Ag, the measured values are well below theoretically expected values based on the rule of mixtures. Such estimates of multiphasic material properties assume perfect interfaces that facilitate maximum load transfer between the different material components. However, if the composite includes weak interfaces, the load transfer will be reduced and therefore the load bearing capacity of the composite will be less than the theoretical resulting in reduced composite modulus compared to theoretical predictions. Although the composite material has lower than expected modulus, its value is still significantly higher than the Young's moduli of traditional "composite electrodes" varying between 0.2 and 0.7 GPa [10]. Since the modulus was increased by two orders of magnitude, a significant increase in the strength is also expected. The latter increased by an order of magnitude as compared to strength values of 4 MPa reported for traditional composite electrodes and are attributed to rather limited ductility. Limited ductility may be attributed to relatively weak interfaces in the material. To the best knowledge of the authors, the strength and Young's modulus of the sintered LTO–LLTO–Ag electrode composite are the highest values reported to date. This novel design may serve as the basis for future high-strength battery designs.

4. Conclusions

An all-solid-state LTO–LLTO–Ag electrode was fabricated via sintering of the corresponding powder. The density of the resultant electrode composite was greater than 97%. The strength and Young's modulus of the electrode are the highest reported values to date, being at least one order of magnitude higher than the corresponding value of traditional "composite electrodes". The sintered LTO–LLTO–Ag electrodes also exhibit reasonable electrochemical properties. Theoretical capacity was achieved during the first cycle. Approximately 85% of the theoretical capacity remained after 10 cycles. The achievement of full capacity was attributed to the 3D percolating network of solid electrolyte and metal, which provide paths for ionic and electronic transport. The type of electrode design demonstrated here may serve as the basis for future high-strength batteries.

Acknowledgements

The authors would like to acknowledge the support from the National Science Foundation Division of Materials Research's Ceramics Program under contract DMR# 0906874. IC would like to acknowledge the Air Force Office of Scientific Research for financial support through a MURI Grant FA9550-06-1-0326 to the University of Washington. SEM and XRD experiments were carried out in the Frederick Seitz Materials Research Laboratory Central Facilities, University of Illinois, which are partially supported by the U.S. Department of Energy under grants DE-FG02-07ER46453 and DE-FG02-07ER46471.

References

[1] J.M. Tarascon, M. Armand, Nature 414 (2001) 359–367.
[2] M. Wakihara, Mater. Sci. Eng. R 33 (2001) 109–134.
[3] D.L. Greene, K.G. Duleep, W.S. McManus, Future Potential of Hybrid and Diesel Powertrains in the US Light-Duty Vehicle Market, Oak Ridge National Laboratory, Oak Ridge, Tennessee, 2004.
[4] E.J. Cairns, P. Albertus, Annu. Rev. Chem. Biomol. Eng. 1 (2010) 299–320.
[5] M.A. Kromer, J.B. Heywood, SAE Int. J. Eng. 1 (2009) 372–391.
[6] J.P. Thomas, M.A. Qidwai, JOM 57 (2005) 18–24.
[7] R.J. Brodd, K. Tagawa, in: W.A. Van Schalkwijk, B. Scrosati (Eds.), Advances in Lithium-Ion Batteries, Kluwer Academic/Plenum Publishers, New York, 2002, pp. 267–275.
[8] P.R. Shearing, L.E. Howard, P.S. Jørgensen, N.P. Brandon, S.J. Harris, Electrochem. Commun. 12 (2010) 374–377.
[9] P.L. Taberna, S. Mitra, P. Poizot, P. Simon, J.-M. Tarascon, Nat. Mater. 5 (2006) 567–573.
[10] H.H. Zheng, G. Liu, X.Y. Song, D. Cheung, P. Ridgway, V. Battaglia, 217th ECS meeting, Vancouver, BC, Canada, 2009, Abs. 0211.
[11] I. Yoshiyuki, L.Q. Chen, I. Mitsuru, N. Tetsurimage, U. Takashi, I. Hiromasa, W. Masataka, Solid State Commun. 86 (1993) 689–693.
[12] H. Aono, E. Sugimoto, Y. Sadaoka, N. Imanaka, G.-Y. Adachi, J. Electrochem. Soc. 136 (1989) 590–591.
[13] A. Sakuda, A. Hayashi, M. Tatsumisago, J. Power Sources 195 (2010) 599–603.
[14] Y.H. Rho, K. Kanamura, J. Power Sources 158 (2006) 1436–1441.
[15] N.J. Dudney, Mater. Sci. Eng. B 116 (2005) 245–249.
[16] Y.I. Jang, B.J. Neudecker, N.J. Dudney, Electrochem. Solid State 4 (2001) A74–A77.
[17] K. Takada, T. Inada, A. Kajiyama, H. Sasaki, S. Kondo, M. Watanabe, M. Murayama, R. Kanno, Solid State Ionics 158 (2002) 269–274.
[18] K. Nagata, T. Nanno, J. Power Sources 174 (2007) 832–837.
[19] T. Kobayashi, Y. Imade, D. Shishihara, K. Homma, M. Nagao, R. Watanabe, T. Yokoi, A. Yamada, R. Kanno, T. Tatsumi, J. Power Sources 182 (2008) 621–625.
[20] A. Aboulaich, R. Bouchet, G. Delaizir, V. Seznec, L. Tortet, M. Morcrette, P. Rozier1, J.-M. Tarascon, V. Viallet, M. Dollé1, Adv. Energy Mater. 1 (2011) 179–183.
[21] W. Lai, C.K. Erdonmez, T.F. Marinis, C.K. Bjune, N.J. Dudney, F. Xu, R. Wartena, Y.-M. Chiang, Adv. Mater. 22 (2010) E139–E144.
[22] R.O. Simmons, R.W. Balluffi, Phys. Rev. 119 (1960) 600–605.
[23] R.M. German, Metal Powder Industries Federation, 2nd ed., Princeton, NJ, 1994, pp. 250–270.
[24] G. Taillades, J. Sarradin, J. Power Sources 125 (2004) 199–205.
[25] Q. Chen, I. Chasiotis, C. Chen, A. Roy, Compos. Sci. Technol. 68 (2008) 3137–3144.

[26] H. Wang, Y. Jang, B. Huang, D.R. Sadoway, Y.M. Chiang, J. Electrochem. Soc. 146 (1999) 473–480.
[27] T. Ohzuku, A. Ueda, N. Yamamoto, J. Electrochem. Soc. 142 (1995) 1431–1435.
[28] P. Kubiak, A. Garcia, M. Womes, L. Aldon, J. Olivier-Fourcade, P.-E. Lippens, J.-C. Jumas, J. Power Sources 119–121 (2003) 626–630.
[29] S.H. Huang, Z.Y. Wen, X.J. Zhu, Z.H. Gu, Electrochem. Commun. 6 (2004) 1093–1097.
[30] J. Gao, C. Jiang, J. Ying, C. Wan, J. Power Sources 155 (2006) 364–367.
[31] G.E. Henein, J.E. Hilliard, J. Appl. Phys. 54 (1983) 728–733.